Frequency entrainment for micromechanical oscillator

M. Zalalutdinov,[a] K. L. Aubin, M. Pandey, A. T. Zehnder, R. H. Rand, H. G. Craighead, and J. M. Parpia
Cornell Center for Material Research, Ithaca, New York 14853

B. H. Houston
Naval Research Laboratory, Washington DC 20375

(Received 11 March 2003; accepted 18 August 2003)

We demonstrate synchronization of laser-induced self-sustained vibrations of radio-frequency micromechanical resonators by applying a small pilot signal either as an inertial drive at the natural frequency of the resonator or by modulating the stiffness of the oscillator at double the natural frequency. By sweeping the pilot signal frequency, we demonstrate that the entrainment zone is hysteretic and can be as wide as 4% of the natural frequency of the resonator, 400 times the $1/Q \sim 10^{-4}$ half-width of the resonant peak. Possible applications are discussed based on the wide range of frequency tuning and the power gain provided by the large amplitude of self-oscillations (controlled by a small pilot signal). © *2003 American Institute of Physics.*
[DOI: 10.1063/1.1618363]

Frequency entrainment is one of the most spectacular phenomena in nonlinear vibrations.[1,2] It was discovered in the 17th century by Huygens who remarked that two slightly out of step pendulum-like clocks became synchronized after they were attached to the same thin wooden board. Later, a similar phenomenon (injection locking) was observed in radio-frequency (rf) circuits[3–5] and laser systems.[6,7]

In this letter, we report frequency entrainment observed in a microelectromechanical system (MEMS) in the rf range. Self-sustained vibrations of mushroom-like microfabricated resonators (thin, single-crystal, silicon disk suspended above the wafer by a silicon dioxide pillar at the center) induced by a continuous-wave (cw) laser were reported earlier.[8] Large amplitude ($\sim\lambda/2$ laser light) self-sustained mechanical oscillations spontaneously occur at the fundamental frequency f_0 when the intensity of a cw laser beam focused on the periphery of the disk reaches a critical value $P_{\text{threshold}}$. The self-oscillatory behavior is attributed to the automodulation of the laser-induced thermal stress field that occurs as the disk moves through the interferometric pattern created by incident and reflected laser beams. These spontaneous vibrations are subject to a frequency instability $\Delta f/f_0 \sim 10^{-3}$ observed on a spectrum analyzer as the sporadic motion of a narrow resonant peak.

We can establish full control over the frequency and phase of the self-oscillations of the disk by applying a small periodic perturbation—a ''pilot'' signal—via inertial drive (provided by an ac voltage applied to a piezoelement) at a frequency close to f_0 or by modulating the effective spring constant of the disk by superimposing a small rf component on the laser beam intensity[9] near $2f_0$. As the frequency of the perturbation is tuned close to f_0 or $2f_0$, we readily observe a distinct point when the phase of the self-oscillatory motion gets locked to that of the pilot. On the polar plot display of a network analyzer (referenced by pilot signal), the locking is manifested by a change from a pattern of spirals to a single point. Once synchronized, a wide range of frequency entrainment can be demonstrated by detuning the pilot signal from f_0 (or $2f_0$) while preserving the locked state. There are no frequency beats in the synchronized state: Only vibrations with the pilot frequency exist in the system. In our experiment, the entrainment range $\Delta f/f_0 \sim 4\%$ was demonstrated for a MHz-range oscillator.

The fabrication process for rf disklike resonators (disk diameter 30 μm, thickness $h=0.25$ μm, central SiO_2 pillar 1 μm height, 0.6 μm diameter) has been described elsewhere.[9] The resulting structure (inset in Fig. 1) was attached to a piezoelectric actuator and placed in a vacuum chamber ($P \sim 10^{-7}$ Torr). The motion of the disk was detected interferometrically.[10]

Figure 1 shows the amplitude and frequency of the vibration of the disk as a function of the pilot signal frequency.

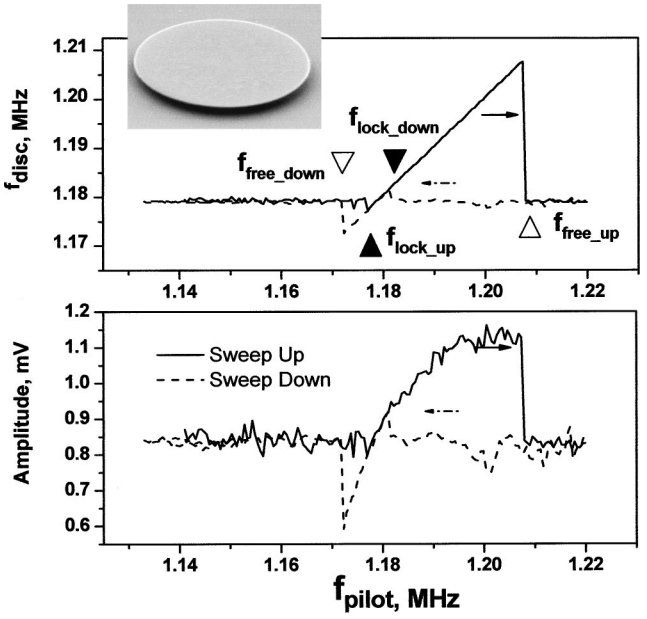

FIG. 1. Frequency and amplitude of the laser-induced self-sustained vibrations as a function of the pilot signal frequency. Laser power $P_{\text{cw}} = 650$ μW, perturbation applied as an inertial drive ($V^{\text{ac}}_{\text{piezo}} = 4$ Vol).

[a]Electronic mail: maxim@ccmr.cornell.edu

Report Documentation Page

Form Approved
OMB No. 0704-0188

1. REPORT DATE	2. REPORT TYPE	3. DATES COVERED
2003		**00-00-2003 to 00-00-2003**

4. TITLE AND SUBTITLE	5a. CONTRACT NUMBER
Frequency entrainment for micromechanical oscillator	5b. GRANT NUMBER
	5c. PROGRAM ELEMENT NUMBER
6. AUTHOR(S)	5d. PROJECT NUMBER
	5e. TASK NUMBER
	5f. WORK UNIT NUMBER
7. PERFORMING ORGANIZATION NAME(S) AND ADDRESS(ES) **Naval Research Laboratory,4555 Overlook Avenue SW,Washington,DC,20375**	8. PERFORMING ORGANIZATION REPORT NUMBER
9. SPONSORING/MONITORING AGENCY NAME(S) AND ADDRESS(ES)	10. SPONSOR/MONITOR'S ACRONYM(S)
	11. SPONSOR/MONITOR'S REPORT NUMBER(S)

12. DISTRIBUTION/AVAILABILITY STATEMENT
Approved for public release; distribution unlimited

13. SUPPLEMENTARY NOTES

14. ABSTRACT

15. SUBJECT TERMS

16. SECURITY CLASSIFICATION OF:			17. LIMITATION OF ABSTRACT	18. NUMBER OF PAGES	19a. NAME OF RESPONSIBLE PERSON
a. REPORT **unclassified**	b. ABSTRACT **unclassified**	c. THIS PAGE **unclassified**		**3**	

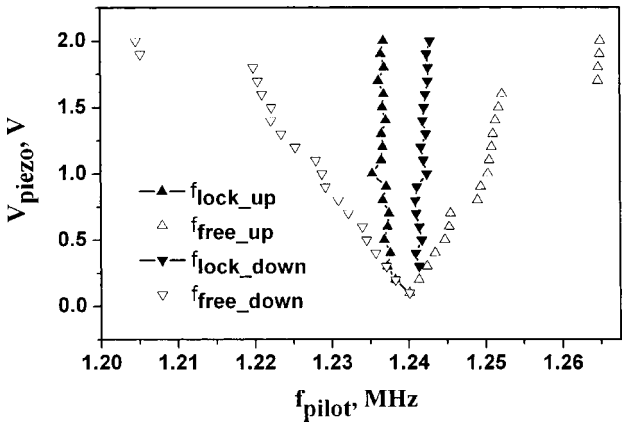

FIG. 2. Entrainment zone as a function of the pilot signal amplitude. Laser power $P_{cw}=1.7$ mW, perturbation applied as an inertial drive. A discontinuity in the width of the entrainment zone at $V_{piezo}\sim 1.8$ V is observed when the expanded entrainment zone overlaps the areas that allow different types of limit-cycle oscillations.

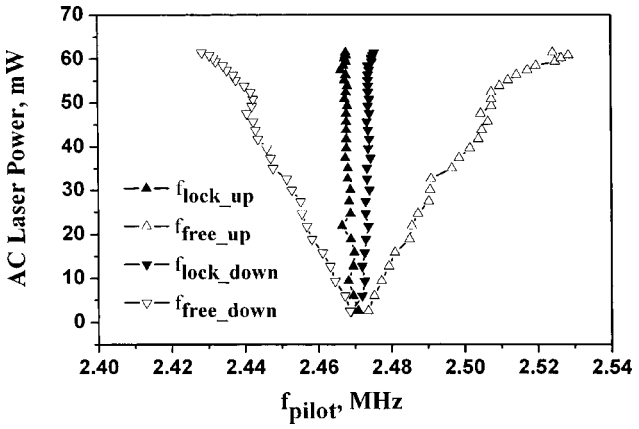

FIG. 3. Entrainment zone as a function of the pilot signal power. Laser power $P_{cw}=1.7$ mW, perturbation applied as a modulation of the secondary laser beam (Ar+) positioned at the center of the disk.

A helium–neon (HeNe) laser beam at $P_{laser}=650\ \mu$W was used to excite the disk into self-oscillation ($P_{threshold}\sim 600\ \mu$W) and an inertial force perturbation was applied by the piezoactuator at frequency f_{pilot}. The solid line represents data acquired while linearly increasing f_{pilot}. After establishing synchronization at $f_{pilot}=f_{lock\_up}$ (~ 2 kHz below f_0), the frequency of the motion follows the change of the pilot frequency. The amplitude of the mechanical motion increases until another critical point is reached (f_{free_up}, 28 kHz above f_0). Synchronization is then broken, self-oscillations at the natural frequency f_0 are restored and for $f_{pilot}>f_{free\_up}$ the pilot signal is ineffective. This general sequence is repeated on a down sweep, except that when entrained at $f_{pilot}<f_{lock\_down}$, the oscillation amplitude is reduced. The critical values of the pilot frequency f_{free} and f_{lock} are different for up and down sweeps, demonstrating the hysteretic behavior of the synchronization for our micromechanical oscillator.

The width of the entrainment range ($f_{lock}-f_{free}$) is determined by the power of the pilot signal. Figure 2 shows an entrainment map where critical points (for up and down sweeps) are plotted as a function of the ac piezovoltage. This plot has a V-shape, consistent with the expectation of zero entrainment range at zero perturbation. Due to the hysteresis, two entrainment areas are present, corresponding to up and down frequency sweeps. These two areas overlap above the natural frequency, creating an ''inner V''—where synchronization to the pilot signal is assured. After establishing phase lock, it is preserved for pilot excursions within the ''outer V''—boundaries marked by f_{free_down} and f_{free_up}, as demonstrated by applying frequency and phase modulation to the pilot signal.

Subharmonic or superharmonic entrainment expected at nf_0 and $(1/n)f_0$ (n is an integer)[11] could be more attractive for applications because the pilot signal and the base frequency are well separated, avoiding parasitic coupling. We failed to demonstrate entrainment with these methods using the inertial drive as a pilot signal. However, a wide range of subharmonic entrainment was observed by partial modulation of the laser beam intensity at $f_{laser}=2f_0$.

Figure 3 shows the map for $2f_0$ entrainment. A cw HeNe laser, $P_{laser}=1.7$ mW was focused on the periphery of the disk to initiate self-oscillations. An Ar^+ ion laser beam modulated at $f_{pilot}\sim 2f_0$ illuminated the area around the pillar providing parametric excitation. The ac component of the Ar^+ laser intensity is plotted as the vertical axis. Hysteretic behavior of the parametric synchronization, similar to that for the inertial-drive entrainment is illustrated by the inner V, i.e., overlap of the entrainment regions from up and down pilot frequency sweeps. The outer V, the range of frequency detuning that still preserves synchronization, is expanded to 70 kHz for 50 μW pilot signal power. Frequency stability of the entrained oscillations seems to be limited by that of the pilot generator. In our case, $\Delta f/f_0\sim 10^{-9}$ was observed.

The analysis of frequency entrainment in our mushroom-like oscillators can be obtained from the differential equations describing self-oscillatory motion:[12]

$$\ddot{z}+\frac{1}{Q}(\dot{z}-D\dot{T})+(1+CT)(z-DT+\beta(z-DT)^3) = M\sin(\omega_{piezo}t), \tag{1}$$

$$\dot{T}=AP_{laser}[1+\varphi\sin(\omega_{mod}t)]\cdot[\alpha+\gamma\sin^2 2\pi(z-z_0)]-BT. \tag{2}$$

The disklike resonator is represented in Eq. (1) as a one degree of freedom oscillator with quality factor Q, temperature-dependent stiffness $(1+CT)$, and nonlinear coefficient β. Time is nondimensionalized by the small amplitude period of vibration. T is the temperature increase under the laser spot and z is the deflection normalized by the laser wavelength λ. The DT terms represent deflection of the disk due to heating. They arise from the slightly bowed (~ 50 nm) equilibrium shape of the disk (a result of the residual stress incorporated in the SOI wafer). The term on the right-hand side of Eq. (1) corresponds to the inertial pilot signal applied by the piezoelement at ω_{piezo}. Equation (2) describes the heat balance for the mushroom. The incident laser power P_{laser} can be partially modulated to produce a pilot signal at a frequency ω_{mod} ($\varphi=$modulation depth). The term in the second set of square brackets describes the portion of the laser power that is actually absorbed by the disk: A constant minimum absorption α, and oscillatory compo-

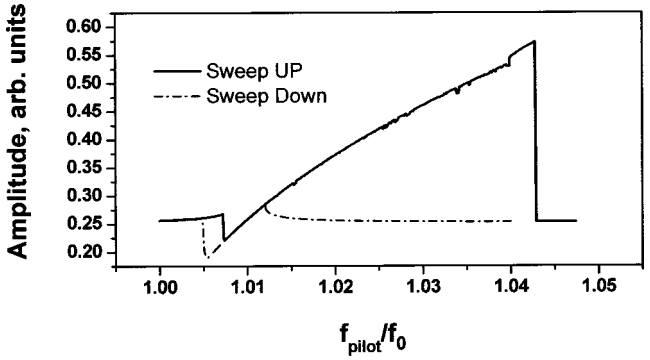

FIG. 4. Result of numerical simulations for the amplitude of the laser-induced self-sustained vibrations as a function of the inertial drive pilot signal frequency ($P_{cw}=650\ \mu W$). The amplitude of inertial drive $M=10^{-4}$, modulation φ in Eq. (2) has been taken as zero.

nent governed by the product of γ and $\sin^2[2\pi(z-z_0)]$ model the absorption determined by the laser light interference between the disk and wafer. The term BT describes thermal relaxation through the pillar. Finite element analysis (FEA) was used to estimate values for the coefficients in Eqs. (1) and (2): $A=0.018\ \mu W^{-1}$, $B=0.488\ K^{-1}$, $C=3.53\times10^{-4}\ K^{-1}$, $D=1.3\times10^{-5}\ K^{-1}$, and $z_0=0.06$ for a mushroom with an outer diameter of 40 μm and a SiO_2 pillar diameter of 6.7 μm. The absorption properties are estimated to be $\alpha=.06$ and $\gamma=.26$. The value of $\beta\approx0.4$ is estimated from measured frequency–amplitude curves.

Figure 4 illustrates sample results of numerical integration for the case of an inertial pilot signal (to be compared with Fig. 1): amplitude $M=10^{-4}$ corresponds to 4 V ac signal applied to piezoactuator, the laser modulation $\varphi=0$. The trajectory of the mechanical motion $z(t)$ for a given frequency of the pilot signal was calculated at each step. The frequency and amplitude of the motion was then determined from the calculated $z(t)$. All of the major features: Synchronization, hysteretic behavior of frequency entrainment, and amplitude dependence of the phase-locked vibrations are demonstrated by the numerical solutions.

Qualitatively, the observed frequency entrainment is similar to the entrainment of a driven Van der Pol limit cycle oscillator.[3,13] The major difference of the wide-range hysteresis of the frequency entrainment observed in our experiments can be explained by the nonlinear behavior of our disk oscillator[11] due to the large amplitude motion. Accordingly, the nonlinearity determined shape of the entrainment zone can be tailored by the cw component of the laser power P_{cw}. The excess of P_{cw} over $P_{threshold}$ enhances the amplitude of self-oscillations and due to hardening of the disk, increases the frequency of the vibrations. The entire entrainment map (Figs. 2 and 3) can be shifted to the left- and right-hand side by adjusting P_{cw}. The asymmetry of the entrainment zone (up versus down frequency detuning), demonstrated by Figs. 1 and 4, is defined by setting P_{cw} just above $P_{threshold}$, where a small frequency decrease will bring the resonator down along the nonlinear amplitude–frequency curve[1] toward zero amplitude and thus break the entrainment. By increasing $P_{cw}\gg P_{threshold}$, one can reach a self-limiting regime[8] when the amplitude of self-oscillations is restricted by the interferometric pattern and is largely decoupled from the frequency. This regime provides a mostly symmetric shape for the entrainment zones illustrated by Figs. 2 and 3.

A detailed study of frequency entrainment in MEMS is in progress in our lab, motivated by possible applications for high-frequency signal processing. Synchronization of limit cycle oscillators by parametric excitation ($2f_0$ laser modulation in our experiment) is the subject of recent theoretical research,[14,15] indicating the possibility for chaotic behavior. A theoretical model was recently proposed for mechanical neurocomputing based on synchronized MEMS oscillators.[16] In wireless devices, for phase or frequency-modulated data transmission, an rf MEMS oscillator, parametrically entrained by a pilot signal from a receiving antenna, would perform as a power amplifier, filter, and frequency down converter. Synchronization could be useful for MEMS applications (for example, optical modulators) requiring wide range yet extremely precise periodic mechanical motion.

In conclusion, synchronization of a rf MEMS limit cycle oscillator was observed by applying a perturbation signal either as a direct drive or as a parametric excitation. A wide range of frequency entrainment (4% of the natural frequency f_0) was observed with pronounced hysteretic behavior attributed to the strong nonlinearity of the resonator. Frequency stability $\Delta f/f_0\sim10^{-9}$ was demonstrated for entrained oscillations and simulated using a simple model.

The authors are grateful to Tuncay Alan for the help with FEA analysis. This work was supported by the Cornell Center for Material Research (CCMR), a Materials Research Science and Engineering Center of the NSF (DMR-0079992). Particular acknowledgment is made of the use of the Research Computing Facility of the CCMR. The authors would also like to acknowledge the Office of Naval Research and DARPA.

[1] A. B. Pippard, *The Physics of Vibration* (Cambridge University Press, Cambridge, UK, 1989), p. 391.
[2] N. Minorsky, *Nonlinear Oscillations*, (Krieger, Malabar, Florida, 1983), p. 438.
[3] Van der Pol, Philos. Mag. **3**, 65 (1927).
[4] M. Golio *The RF and Microwave Handbook* (CRC Press, Boca Raton, FL, 2001), p. 5–98.
[5] L. M. Pecora and T. L. Carroll, Phys. Rev. Lett. **64**, 821 (1990).
[6] M. Poulin, C. Latrasse, D. Touahri, and M. Tetu, Opt. Commun. **207**, 233 (2002).
[7] Y. Liu, P. Davis, Y. Takiguchu, T. Aida, S. Saito, and J.-M. Liu, IEEE J.Quantum Electron. **39**, 269 (2003).
[8] M. Zalalutdinov, A. Zehnder, A. Olkhovets, S. Turner, L. Sekaric, B. Ilic, D. Czaplewski, J. M. Parpia, and H. G. Craighead, Appl. Phys. Lett. **79**, 695 (2001).
[9] M. Zalalutdinov, A. Olkhovets, A. Zehnder, B. Ilic, D. Czaplewski, H. G. Craighead, and J. M. Parpia, Appl. Phys. Lett. **78**, 3142 (2001).
[10] D. Carr and H. Craighead, J. Vac. Sci. Technol. B **15**, 2760 (1997).
[11] C. Hayashi, *Nonlinear Oscillations in Physical Systems* (Princeton University, Princeton, NJ, 1985).
[12] M. Zalalutdinov, J. Parpia, K. Aubin, H. Craighead, T. Alan, A. Zehnder, and R. Rand, Proceedings of 2003 ASME Design Engineering Technical Conferences, 19th Biennial Conference on Mechanical Vibration and Noise, September 2003, Chicago, Illinois, paper no. DETC 2003-48446 (CD-ROM).
[13] R. Rand, *Lecture Notes on Nonlinear Vibrations* available online at http://www.tam.cornell.edu/randdocs/nlvibe45.pdf (2003).
[14] K. Szabelski and J. Warminski, J. Sound Vib. **187**, 595 (1995).
[15] G. Litak, G. Spuz-Spos, K. Szabelski, and J. Warminski, Int. J. Bifurcation Chaos **9**, 493 (1999).
[16] F. Hoppensteadt and E. Izhikevich, IEEE Trans. Circuits Syst., I: Fundam. Theory Appl. **48**, 133 (2001).